Theoretical Investigation of a Spectrally Pure-State Generation from Isomorphs of KDP Crystal at Near-Infrared and Telecom Wavelengths

Rui-Bo Jin,[1,4] Neng Cai,[1] Ying Huang,[1] Xiang-Ying Hao,[1,*] Shun Wang,[1] Fang Li,[1] Hai-Zhi Song,[2,3] Qiang Zhou,[2,5,†] and Ryosuke Shimizu[6]

[1] *Hubei Key Laboratory of Optical Information and Pattern Recognition, Wuhan Institute of Technology, Wuhan 430205, PR China*

[2] *Institute of Fundamental and Frontier Science and School of Optoelectronic Science and Engineering, University of Electronic Science and Technology of China, Chengdu 610054, PR China*

[3] *Southwest Institute of Technical Physics, Chengdu 610041, PR China*

[4] *State Key Laboratory of Quantum Optics and Quantum Optics Devices, Shanxi University, Taiyuan, 030006, PR China*

[5] *CAS Key Laboratory of Quantum Information, University of Science and Technology of China, Hefei 230026, PR China*

[6] *The University of Electro-Communications, 1-5-1 Chofugaoka, Chofu, Tokyo, Japan*

(Received 19 October 2018; revised manuscript received 28 December 2018; published 28 March 2019)

A spectrally uncorrelated biphoton state generated from the spontaneous nonlinear optical process is an important resource for quantum information. Currently, such a spectrally uncorrelated biphoton state can only be prepared from limited kinds of nonlinear media, thus limiting their wavelengths. In order to explore a wider wavelength range, here we theoretically study the generation of a spectrally uncorrelated biphoton state from 14 isomorphs of potassium dihydrogen phosphate (KDP) crystal. We find that 11 crystals from the "KDP family" still maintain similar nonlinear optical properties of KDP, such as KDP, DKDP, ADP, DADP, ADA, DADA, RDA, DRDA, RDP, DRDP, and KDA, which satisfy three kinds of the group-velocity matching conditions for spectrally uncorrelated biphoton-state generation from near-infrared to telecom wavelengths. Based on the uncorrelated biphoton state, we investigate the generation of a heralded pure-state single photon by detecting one member of the biphoton state to herald the output of the other. The purity of the heralded single photon is as high as 0.98 without using a narrow-band filter; the Hong-Ou-Mandel interference from independent sources can also achieve a visibility of 98%. This study may provide more and better single-photon sources for quantum-information processing at near-infrared and telecom wavelengths.

DOI: 10.1103/PhysRevApplied.11.034067

I. INTRODUCTION

Single photons are essential quantum-information carriers for photonics quantum-information processing (QIP), because one can easily manipulate, transmit, and detect single photons, and then can implement many QIP protocols. A common method to prepare single photons is based on the generation of the biphoton state (usually named idler and signal photons) followed by the detection of one member of the pair (for instance, the idler), which heralds the output of the other [1–3]. In this scheme, a crucial step is the pair-generation process, which can be achieved through spontaneous parametric down-conversion (SPDC) or spontaneous four-wave mixing (SFWM) in a nonlinear optical medium. The SPDC is a widely used method for the generation of correlated pairs of photons. In the SPDC process, a higher-energy pump photon is "split" into the signal and idler biphotons, which are generally spectrally correlated due to the energy and momentum conservation laws. For many QIP applications like quantum computation [4] or boson sampling [5], it is necessary to utilize biphotons with no spectral correlations to obtain the heralded pure-state single photon, so as to achieve high distinguishability, i.e., high-visibility Hong-Ou-Mandel (HOM) interference [6], between independent single photon sources [7–9]. A high HOM interference visibility corresponds to a high operation fidelity for several QIP protocols, such as quantum teleportation [10] and measurement-device-independent quantum key distribution (MDI QKD) [11, 12]. Therefore, it is very important to prepare spectrally uncorrelated biphotons from the SPDC process.

Two methods can be applied to remove the spectral correlations between the signal and idler photons. The

*xyhao.321@163.com
†zhouqiang@uestc.edu.cn

first one is the filtering method, in which the spectral uncorrelated biphoton state is obtained by simply and directly filtering the correlated ones using narrow bandpass filters. However, this method may not only severely decrease the brightness of the photon source, but also introduce extra noises [7,13]. The second one is the quantum-state-engineering method [14–16], in which, by engineering the group-velocity-matched (GVM) condition, the spectrally uncorrelated biphoton state can be intrinsically generated in specific crystals at several fixed wavelengths. For example, the KDP crystal at 830 nm has a maximal purity of 0.97 [7–9]; the β barium borate (BBO) crystal at 1514 nm can achieve a maximal purity of 0.82 [14,17–19]; the periodically poled KTP crystal (PPKTP) at 1584 nm has a maximal purity of 0.82 [20–36] and this high purity can be kept when the wavelength is tuned from 1400 to 1700 nm [37]. The purity for PPKTP crystals can be further improved from 0.82 to near 1 using the custom poling crystal [38–42]. Such a GVM condition can also be satisfied in the SFWM process in optical fiber with birefringence [43,44].

As described above, the spectrally uncorrelated biphoton state is an important but rare resource. At present, researchers have only used limited kinds of crystals (KDP, BBO, PPKTP, etc) to produce such a biphoton state in a limited wavelength range. It should be valuable to find more crystals to prepare the spectrally uncorrelated biphoton state, than to prepare the heralded pure-state single photon in a wider wavelength range. Recently, we have found that four isomorphs of PPKTP (PPRTP, PPKTA, PPRTA, PPCTA) can retain the properties of PPKTP, i.e, these isomorphs satisfy the GVM condition and can prepare the spectrally uncorrelated biphoton state in the range of 1300 to 2100 nm [45–47].

In this work, inspired by the previous studies, we investigate the possibility of the generation of the spectrally uncorrelated biphoton state from 14 isomorphs from the "KDP family". This paper is organized as follows. First, the introductory part provides the background and motivation of this research. Second, the theoretical part introduces the basic characteristics of KDP isomorphous crystals, and the principle of spectrally uncorrelated biphoton-state generation based on GVM conditions. Third, the simulation part shows the wavelength degenerate case, nondegenerate case, and the Hong-Ou-Mandel (HOM) interference patterns with an independent heralded spectrally pure single-photon state. Fourth, we provide fruitful discussions on the simulation results in the discussion section. Finally, we summarize the paper in the conclusion section.

II. THEORY

A. The basic characteristics of the "KDP family"

The general form of the isomorphs of KDP can be written as MDX or DMDX with $M = \mathrm{K, Rb, Cs, NH_4}$ and $X = \mathrm{P, As}$. Here, K, Rb, Cs are alkali metal elements of group IA in the periodic table; P and As are elements of group VA in the periodic table; and the meaning of the first letter D in DMDX is to replace the protium element in MDX with deuterium. These crystals include KDP (KH_2PO_4), DKDP (KD_2PO_4), ADP ($NH_4H_2PO_4$), DADP ($ND_4D_2PO_4$), ADA ($NH_4H_2AsO_4$), DADA ($ND_4D_2AsO_4$), RDA (RbH_2AsO_4), DRDA (RbD_2AsO_4), RDP (RbH_2PO_4), DRDP (RbD_2PO_4), KDA (KH_2AsO_4), DKDA (KD_2AsO_4), CDA (CsH_2AsO_4), and DCDA (CsD_2AsO_4) [48,49]. All of these 14 crystals belong to the "KDP family" and have similar properties to the KDP crystal: (1) all of them are negative uniaxial crystal ($n_o > n_e$, point group $\bar{4}2m$); (2) all of them have a high-transmission rate from ultraviolet to infrared; (3) all of them have a high-optical-damage threshold; (4) all of them are widely used in lasers, optical switches, electro-optic modulators, etc.

B. The principle of spectrally uncorrelated biphoton-state generation based on GVM condition

The biphoton state $|\psi\rangle$ generated from the process of SPDC can be written as

$$|\psi\rangle = \int_0^\infty \int_0^\infty d\omega_s\, d\omega_i f(\omega_s, \omega_i)\hat{a}_s^\dagger(\omega_s)\hat{a}_i^\dagger(\omega_i)|0\rangle|0\rangle, \tag{1}$$

where ω is the angular frequency; the subscripts s and i indicate the signal and idler photon; $\hat{a}^\dagger$ is the creation operator. The joint spectral amplitude (JSA) $f(\omega_s, \omega_i)$ is the product of the pump-envelope function (PEF) $\alpha(\omega_s, \omega_i)$ and the phase-matching function (PMF) $\phi(\omega_s, \omega_i)$, i.e.,

$$f(\omega_s, \omega_i) = \alpha(\omega_s, \omega_i) \times \phi(\omega_s, \omega_i). \tag{2}$$

A PEF with a Gaussian distribution can be written as [50]

$$\alpha(\omega_s, \omega_i) = \exp\left[-\frac{1}{2}\left(\frac{\omega_s + \omega_i - \omega_p}{\sigma_p}\right)^2\right], \tag{3}$$

where σ_p is the bandwidth of the pump. Using wavelengths as the variables, the PEF can be rewritten as

$$\alpha(\lambda_s, \lambda_i) = \exp\left(-\frac{1}{2}\left\{\frac{1/\lambda_s + 1/\lambda_i - 1/(\lambda_0/2)}{\Delta\lambda/[(\lambda_0/2)^2 - (\Delta\lambda/2)^2]}\right\}\right), \tag{4}$$

where $\lambda_0/2$ is the central wavelength of the pump; $\Delta\lambda$ is the bandwidth in wavelength and σ_p is

$$\sigma_p = \frac{2\pi c\Delta\lambda}{(\lambda_0/2)^2 - (\Delta\lambda/2)^2}, \tag{5}$$

where c is the speed of light. By assuming a flat phase distribution, the PMF function can be written as [50]

$$\phi(\omega_s, \omega_i) = \mathrm{sinc}\left(\frac{\Delta kL}{2}\right), \tag{6}$$

where L is the length of crystal, $\Delta k = k_p - k_i - k_s$ and $k = 2\pi n(\lambda, \varphi)/\lambda$ is the wave vector. For ordinary ray (o ray), the refractive index $n_o(\lambda)$ is a function of wavelength λ. While for extraordinary ray (e ray), the refractive index $n_e(\lambda, \varphi)$ is a function of φ and wavelength λ. φ is the angle between the optical axis of the crystal and the direction of the pump laser. In this study, the pump and idler are e rays, and the signal is o ray. Then, Δk can be rewritten as

$$\Delta k = 2\pi\left[\frac{n_e(\lambda_p, \varphi)}{\lambda_p} - \frac{n_o(\lambda_s)}{\lambda_s} - \frac{n_e(\lambda_i, \varphi)}{\lambda_i}\right]. \tag{7}$$

While the phase mismatch is zero, i.e., $\Delta k = 0$, the phase is completely matched, therefore, it is called the phase-matching condition. The angle between the positive direction of the horizontal axis and the ridge direction of the PEF is always 135° [37]. In contrast, the angle θ between the horizontal axis and the ridge of the PMF is determined by the following equation [37]:

$$\tan\theta = -\left[\frac{V_{g,p}^{-1}(\omega_p) - V_{g,s}^{-1}(\omega_s)}{V_{g,p}^{-1}(\omega_p) - V_{g,i}^{-1}(\omega_i)}\right], \tag{8}$$

where $V_{g,\mu} = d\omega/dk_\mu(\omega) = 1/k'_\mu(\omega), (\mu = p, s, i)$ is the group velocity of the pump, the signal and the idler. In other words, the shape of the PMF is determined by the GVM condition. We consider three kinds of GVM conditions in this work [16]. The first GVM condition (GVM_1) is

$$V_{g,p}^{-1}(\omega_p) = V_{g,s}^{-1}(\omega_s). \tag{9}$$

The second GVM condition (GVM_2) is

$$V_{g,p}^{-1}(\omega_p) = V_{g,i}^{-1}(\omega_i). \tag{10}$$

The third GVM condition (GVM_3) is

$$2V_{g,p}^{-1}(\omega_p) = V_{g,s}^{-1}(\omega_i) + V_{g,s}^{-1}(\omega_s). \tag{11}$$

When the GVM_1, GVM_2, or GVM_3 conditions are satisfied, $\varphi = 0°$, 90°, or 45°, respectively. With these three kinds of GVM conditions, it is possible to prepare spectrally uncorrelated biphotons. In the next section, we calculate the parameters for GVM conditions in detail [51].

III. SIMULATION

A. Wavelength degenerate case

First, we consider the type-II ($e \to o + e$) SPDC with collinear and wavelength-degenerated ($2\lambda_p = \lambda_s = \lambda_i$) configurations. According to GVM conditions, the GVM wavelength $\lambda_{p(s,i)}$ and the corresponding phase-matched angle φ can be calculated. As an example, Fig. 1 shows the PMF and $\mathrm{GVM}_{1(2,3)}$ conditions for different wavelengths and phase-matched angles for ADP crystal. The cross points correspond to the case where PMF and GVM conditions are simultaneously satisfied. Following a similar method, we can also calculate the GVM conditions for other crystals. Table I lists the details of the three kinds of GVM conditions for 11 crystals from the "KDP family". In Table I, the down-converted photons have a wavelength range from 822 to 1830 nm, and the corresponding pump wavelength range is from 411 to 915 nm. The purity, a parameter to characterize the spectral correlations of the biphotons, can be numerically calculated by conducting a Schmidt decomposition on the JSA, i.e., $f(\omega_1, \omega_2)$—see more details in Ref. [37].

The maximal purities are around 0.97 for photon pairs generated from GVM_1 and GVM_2 conditions, and 0.82 for the case of the GVM_3 condition. Our analysis indicates these "KDP family" crystals can be used to generate the spectrally uncorrelated biphoton state.

In order to investigate more details of the GVM conditions, we choose six typical configurations from Table I and plot their JSAs. The results are shown in Figs. 2(a)–2(f). Figures 2(a) and 2(d) in the first column show the JSAs of the GVM_1 condition, which has a long-strip shape in the horizontal direction. Here, we set the

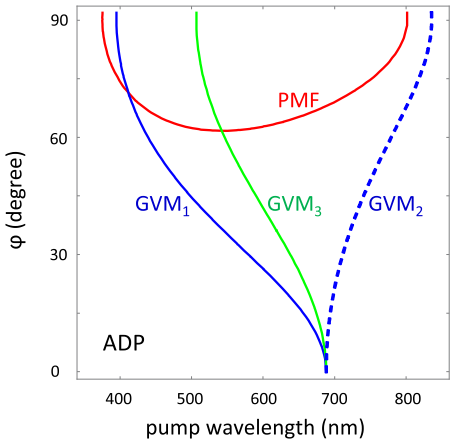

FIG. 1. The phase-matched function (PMF) and group-velocity-matched functions (GVM_1, GVM_2, and GVM_3) for different pump wavelengths λ and phase-matched angle φ for ADP crystal. In this calculation, we consider the type-II ($e \to o + e$) condition with collinear and wavelength-degenerated ($2\lambda_p = \lambda_s = \lambda_i$) configuration.

TABLE I. Three kinds of GVM conditions for 11 crystals. $\lambda_{p(s,i)}$ is the GVM wavelength for the pump (signal, idler). φ is the phase-matched angle and d_{eff} is the effective nonlinear coefficient. The d_{eff} values are taken from the SNLO *v*66 software package, developed by AS-Photonics, LLC [52]. Some of the d_{eff} values are not available in this software. The Sellmeier equations are obtained from Refs. [48] and [49]. Note that CDA and DCDA do not satisfy the GVM condition; the Sellmeier equation of DKDA has not been reported yet.

Name	GVM_1 (purity ≈ 0.97)	GVM_2 (purity ≈ 0.97)	GVM_3 (purity ≈ 0.82)
KDP	$\lambda_p = 415$ nm, $\lambda_{s,i} = 830$ nm $\varphi = 67.7°$, $d_{\text{eff}} = 0.28$ pm/V	Not satisfied	$\lambda_p = 551$ nm, $\lambda_{s,i} = 1102$ nm $\varphi = 59.0°$, $d_{\text{eff}} = 0.33$ pm/V
DKDP	$\lambda_p = 476$ nm, $\lambda_{s,i} = 952$ nm $\varphi = 57.6°$, $d_{\text{eff}} = 0.22$ pm/V	$\lambda_p = 915$ nm, $\lambda_{s,i} = 1830$ nm $\varphi = 62.9°$, $d_{\text{eff}} =$ unknown	$\lambda_p = 626$ nm, $\lambda_{s,i} = 1252$ nm $\varphi = 51.7°$, $d_{\text{eff}} = 0.34$ pm/V
ADP	$\lambda_p = 411$ nm, $\lambda_{s,i} = 822$ nm $\varphi = 71.2°$, $d_{\text{eff}} = 0.34$ pm/V	Not satisfied	$\lambda_p = 541$ nm, $\lambda_{s,i} = 1082$ nm $\varphi = 61.5°$, $d_{\text{eff}} = 0.44$ pm/V
DADP	$\lambda_p = 464$ nm, $\lambda_{s,i} = 978$ nm $\varphi = 59.6°$, $d_{\text{eff}} = 0.45$ pm/V	$\lambda_p = 869$ nm, $\lambda_{s,i} = 1738$ nm $\varphi = 64.2°$, $d_{\text{eff}} =$ unknown	$\lambda_p = 609$ nm, $\lambda_{s,i} = 1218$ nm $\varphi = 53.2°$, $d_{\text{eff}} = 0.48$ pm/V
ADA	$\lambda_p = 461$ nm, $\lambda_{s,i} = 922$ nm $\varphi = 69.8°$, $d_{\text{eff}} = 0.26$ pm/V	Not satisfied	$\lambda_p = 605$ nm, $\lambda_{s,i} = 1210$ nm $\varphi = 60.6°$, $d_{\text{eff}} =$ unknown
DADA	$\lambda_p = 522$ nm, $\lambda_{s,i} = 1044$ nm $\varphi = 57.0°$, $d_{\text{eff}} = 0.33$ pm/V	Not satisfied	$\lambda_p = 741$ nm, $\lambda_{s,i} = 1482$ nm $\varphi = 49.5°$, $d_{\text{eff}} =$ unknown
RDA	Not satisfied	Not satisfied	$\lambda_p = 648$ nm, $\lambda_{s,i} = 1296$ nm $\varphi = 72.5°$, $d_{\text{eff}} = 0.21$ pm/V
DRDA	$\lambda_p = 546$ nm, $\lambda_{s,i} = 1092$ nm $\varphi = 74.1°$, $d_{\text{eff}} = 0.20$ pm/V	Not satisfied	$\lambda_p = 727$ nm, $\lambda_{s,i} = 1454$ nm $\varphi = 62.8°$, $d_{\text{eff}} = 0.29$ pm/V
RDP	Not satisfied	Not satisfied	$\lambda_p = 578$ nm, $\lambda_{s,i} = 1156$ nm $\varphi = 82.1°$, $d_{\text{eff}} = 0.10$ pm/V
DRDP	Not satisfied	Not satisfied	$\lambda_p = 639$ nm, $\lambda_{s,i} = 1278$ nm $\varphi = 70.0°$, $d_{\text{eff}} = 0.21$ pm/V
KDA	$\lambda_p = 467$ nm, $\lambda_{s,i} = 934$ nm $\varphi = 68.7°$, $d_{\text{eff}} = 0.40$ pm/V	Not satisfied	Not satisfied

crystal length $L = 15$ mm and the pump bandwidth $\Delta\lambda = 2$ nm. The degenerated wavelengths for KDP and ADP are 830 and 822 nm, respectively. These wavelengths are the typical near-infrared wavelength, where silicon APD has high detecting efficiency. Figures 2(b) and 2(e) in the second column show the JSAs of the GVM_2 condition, which has a long-strip shape in the vertical direction. Here, we set the crystal length $L = 30$ mm and the pump bandwidth $\Delta\lambda = 3$ nm. The purity is 0.96 for DADA and 0.98 for ADP. The degenerated wavelength for DADA and ADP are 1560 and 1622 nm, respectively. These wavelengths are the typical telecom wavelength. The purity is 0.96 for DKDP and 0.97 for DADP. The degenerated wavelength for DKDP and DADP are 1830 and 1738 nm, respectively. Figures 2(c) and 2(f) in the third column show the JSAs of the GVM_3 condition, which has a near-round shape in the center and with side lobes in the antidiagonal directions. For the GVM_3 condition, the tunable range in wavelength is very wide. So, without degradation of the purity, we can shift the wave length for DADA from 1482 (GVM_3 wavelength in Table I) to 1500 nm [in Fig. 2(c)], which is in the S band in telecom wavelength. The wavelength of DRDA crystal can also be shifted from 1454 (GVM_3 wavelength in Table I) to 1500 nm in Fig. 2(f). This wide tunability is the same as the case of PPKTP crystal, which has a wavelength tunable range of more than 200 nm, while keeping the purity around 0.82 [37].

All the JSAs in Figs. 2(a)–2(f) and Table I have high spectral purities, indicating that the isomorphs of KDP retain the KDP-like properties. Furthermore, it also can be seen that the wavelengths, at which the spectrally uncorrelated biphoton state can be generated, range from 822 to 1830 nm with different crystals. This shows that isomorphs of KDP can extend the wavelength range for spectrally uncorrelated biphoton-state generation.

B. Wavelength nondegenerate case

In the nondegenerate case, we consider the wavelength of the pump photons located at approximately 400–540 nm, which are the wavelengths for commercially available, low-cost laser diodes; One of the down-converted photons is at the approximately 500–900 nm wavelength range, where the silicon avalanche photodiode (APD) has good detection performance; The other down-converted photon is at the telecom wavelength around 1550 nm, for low-loss long-distance transmission in optical fibers. The typical configurations include 405 nm $\rightarrow$ 548 nm + 1550 nm, 450 nm $\rightarrow$ 635 nm + 1550 nm, 520 nm $\rightarrow$ 783 nm + 1550 nm and 530 nm $\rightarrow$ 806 nm + 1550 nm. These configurations are connecting the near-infrared wavelength and the telecom wavelength [53,54].

Calculation results show that 3 out of the 11 crystals can satisfy the GVM_1 condition in a type-II ($e \rightarrow o + e$) SPDC

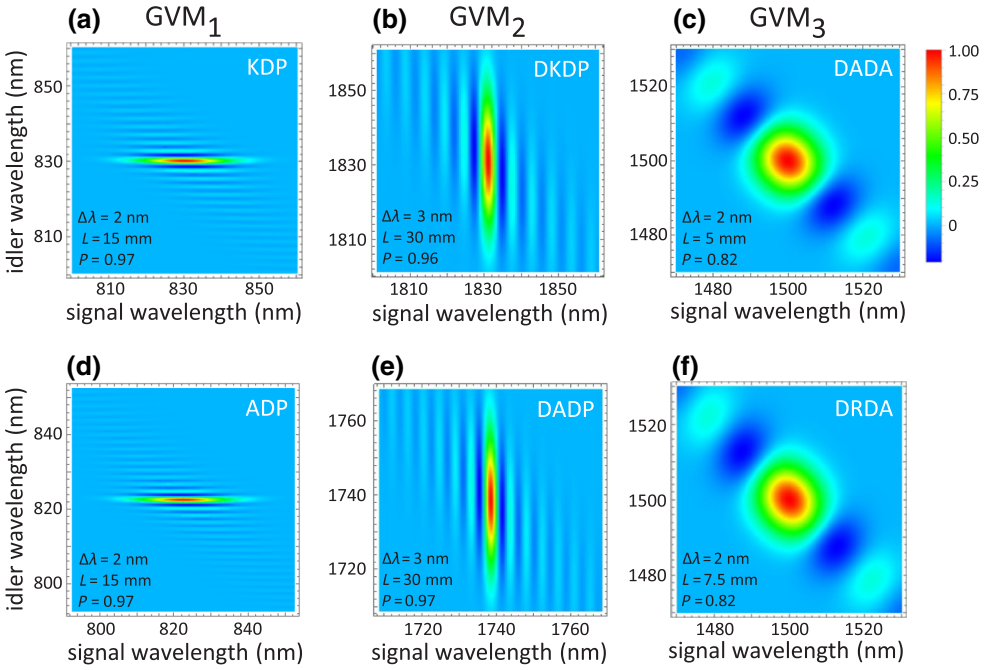

FIG. 2. The JSA of biphotons generated from the isomorphs of KDP. The bandwidth $\Delta\lambda$, the crystal length L, and the purity P are listed in each figure. Figures (a),(d) in the first column are for the GVM_1 condition. Figures in the second and third columns are for GVM_2 and GVM_3 conditions, respectively.

with collinear and wavelength-nondegenerated ($\lambda_s \neq \lambda_i$) configurations. Table II lists the GVM_1 conditions for RDA, DRDP, and KDA, and the JSAs under these conditions are shown in Figs. 3 and 4(a). All the JSAs in Figs. 3 and 4(a) have high purities of 0.97 to 0.98.

C. HOM interference between independent sources

Based on the generation of the spectrally uncorrelated biphoton state, we can obtain heralded pure-state single photons. For example, using one KDA crystal, we can produce a signal (s_1) and idler (i_1) photon pair. We keep s_1 as the heralded single photon, while detecting i_1 by a single-photon detector (SPD), and use the output of the SPD as the heralding signal of the output of s_1. Next, we verify the indistinguishability of generated heralded single photons, which is realized by checking the Hong-Ou-Mandel (HOM) interference [6] with two independent heralded single-photon sources, with a typical experimental setup shown in Refs. [7,23]. In this interference, two signals s_1 and s_2 are sent to a beamsplitter for interference, and two idlers i_1 and i_2 are detected by SPDs for heralding the signals. The fourfold coincidence counts P as a function of τ can be described by Eq. (12) [55],

$$P(\tau) = \frac{1}{4}\int_0^\infty\int_0^\infty\int_0^\infty\int_0^\infty d\omega_{s_1} d\omega_{s_2} d\omega_{i_1} d\omega_{i_2} \left| f_1(\omega_{s_1},\omega_{i_1}) f_2(\omega_{s_2},\omega_{i_2}) - f_1(\omega_{s_2},\omega_{i1}) f_2(\omega_{s_1},\omega_{i_2}) e^{-i(\omega_{s_2}-\omega_{s_1})\tau}\right|^2, \quad (12)$$

where f_1 and f_2 are the JSAs from the first and the second crystals.

Figure 4(a) is the JSA of the biphoton state from KDA crystal, with crystal length $L = 15$ mm and a pump bandwidth of $\Delta\lambda = 2$ nm. Under this condition, the spectral purity is as high as 0.98. Figures 4(b) and 4(c) are the HOM interference curves between two heralded signals or two heralded idlers. Without using any narrow bandpass filters, the visibility can achieve 98%. Please note that the visibility is equal to the purity for the ideal case in the HOM interference between independent sources [7,23,56].

IV. DISCUSSIONS

A purity of 98% is a good metric in our investigation, but it may need to be even higher for practical applications,

TABLE II. The parameters of three crystals. φ is the phase-matched angle and d_{eff} is the effective nonlinear coefficient. The d_{eff} values are taken from the SNLO *v*66 software package, developed by AS-Photonics, LLC [52]. Some of the d_{eff} values are not available in this software.

Name	GVM_1 condition
RDA	$\lambda_p = 520$ nm, $\lambda_s = 764$ nm, $\lambda_i = 1630$ nm, $\varphi = 56.0^\circ$, d_{eff} = unknown
DRDP	$\lambda_p = 500$ nm, $\lambda_s = 744$ nm, $\lambda_i = 1526$ nm, $\varphi = 56.0^\circ$, d_{eff} = unknown
KDA	$\lambda_p = 520$ nm, $\lambda_s = 787$ nm, $\lambda_i = 1531$ nm, $\varphi = 45.1^\circ$, $d_{\text{eff}} = 0.52$ pm/V

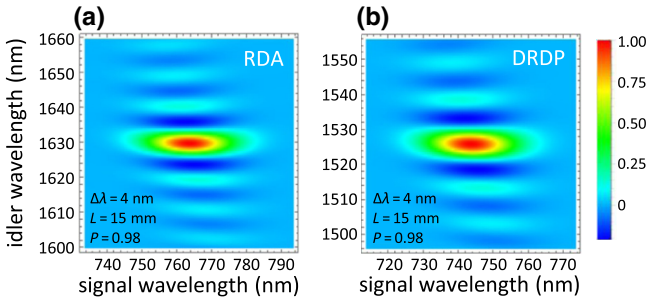

FIG. 3. The JSA of biphotons generated from RDA and DRDP. The center wavelengths are set to be the GVM wavelength in Table II for each crystal. The pump bandwidth $\Delta\lambda = 4$ nm and the crystal length $L = 15$ mm.

e.g., for cascaded operations, or for high-fidelity quantum-information processing. Purity higher than 98% may be realized by inserting a coarse bandpass filter, or adopting waveguide structure. In particular, utilizing the geometry dispersion in a waveguide structure also has other advantages such as single spatial mode, high brightness, on-chip integration, etc. For instance, in the pioneering work from Spring *et al.*, they demonstrated a near-identical pure-photon source based on a silica chip [57].

For experimental realization, the working regime required by our calculation can be straightforwardly realized. For example, the center wavelength of the pump can be accurately controlled by utilizing a wavelength-tunable Ti:sapphire laser; the bandwidth of the pump can be manipulated by using a bandpass filter; the crystals with the required conditions (including the crystal length and the cutting angle) are also commercially available.

In our work, we also try CDA and DCDA, but these two crystals do not satisfy the GVM condition and, therefore, cannot be used for spectrally uncorrelated biphoton-state preparation. One possible reason for this situation is that these crystals may have some special properties, therefore, they do not maintain the properties of KDP. It could also be the reason for the inaccurate test of the Sellmeier equations for these crystals in previous experiments. In addition, the Sellmeier equation of DKDA crystal has not been reported. We would also like to point out that our theoretical expectations can be easily verified experimentally by measuring the JSA of the generated biphoton states [7,8].

Our current work only discusses some pure-element crystals. It is possible to mix these elements to obtain mixed crystals, for example, the KADP crystal [58]. The mixed crystal may also maintain the properties of the KDP and it is worth making further investigations in the future. If the deuterium element is replaced by tritium, we may obtain a series of new isomorphic crystals TMDX ($M = \mathrm{K, Rb, Cs, NH_4}$; $X = \mathrm{P, As}$), which may have novel nonlinear optical properties in the GVM wavelengths, nonlinear coefficients, damage threshold, etc. It is also possible to mix three isotopes of hydrogen, i.e., protium, deuterium, and tritium, so as to make mixed crystal for better performance in nonlinear optics.

In this paper, we only consider the collinear matched SPDC. For noncollinear matching, the satisfied wavelength range can be further expanded, and one can greatly increase the wavelength range of the spectrally uncorrelated biphoton state, thus for the heralded pure-state single-photon source.

For future applications, the biphotons in Figs. 2(a) and 2(d) can be applied for near-infrared wavelength; Figs. 2(c) and 2(f) are useful for the telecom wavelength; Figs. 3 and 4(a) are good candidates for connecting the near-infrared wavelength and telecom wavelength, which may have great potential in quantum networks [59]. Figures 2(a), 2(b), 2(d), 2(e), 3, and 4(a) can be used for interference between two signals from two independent SPDC sources. Figures 2(c) and 2(f) are useful for interference between the signal and idler photons from one SPDC source. The highly pure single-photon sources at telecom wavelengths are very important for practical applications, which require long-distance transmission in low-loss and low-cost optical fibers, for example, for quantum-key distribution [60], quantum-digital signature [61], quantum direct communication [62], quantum teleportation [63], quantum networks [64], etc.

Although the nonlinear coefficients of the "KDP family" are generally lower than that of BBO and PPKTP, the KDP isomorph crystals have their own advantages and can not be easily replaced. For instance, the KDP family can achieve the maximal spectral purity of 0.98, much

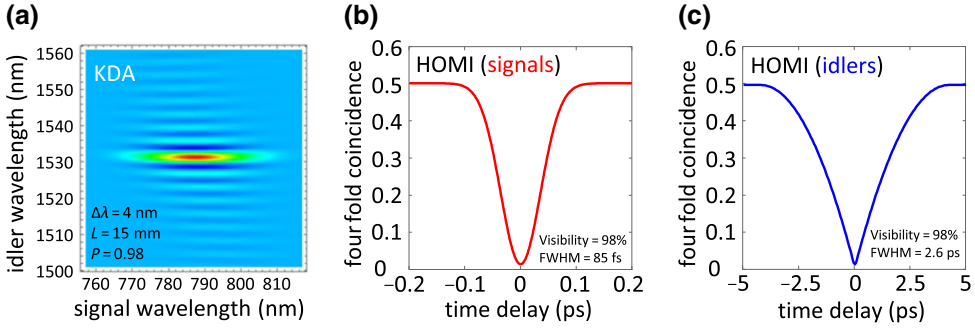

FIG. 4. (a) The JSA of the biphoton generated from KDA; (b) HOM interference curve with two heralded signal photons from two independent DKDP sources; (c) HOM interference curve with two heralded idler photons.

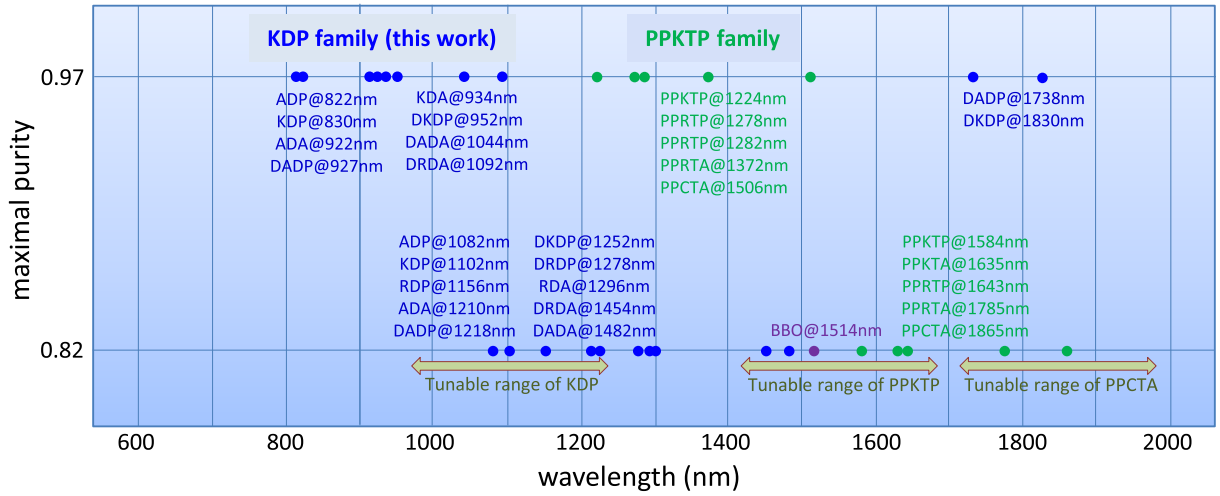

FIG. 5. The wavelength versus achievable maximal spectral purity for different GVM-matched crystals. The "KDP family" (blue points) can achieve purity of 0.97 from 822 to 1830 nm, and 0.82 from 1082 to 1482 nm. The BBO crystal (purple point) can achieve purity of 0.82 at 1514 nm [14,17,18]. The "PPKTP family" (green points) can achieve purity of 0.97 from 1224 to 1506 nm, and 0.82 from 1584 to 1865 nm. For the GVM_3 condition, the purity of 0.82 can be kept when the wavelength is tuned for more than 200 nm.

higher than the value of 0.82 by the BBO [14,17,18], as summarized in Fig. 5. The size of DKDP crystals can achieve 900 mm [65], much larger than the typical size of $1 \times 2 \times 30$ mm^3 for PPKTP [37]. The large size, fast growth rate, and high damage thresholds make KDP useful for laser nuclear fusion in the National Ignition Facility [65]. Historically, the first SPDC experiment was realized in ADP crystal [66], and later several important experiments were also realized in KDP crystals [7,8,50]. We expect that our investigated 11 kinds of isomorphs from the "KDP family" will also have wide applications in the future.

V. CONCLUSION

By theoretical calculation and numerical simulation, we investigate the preparation of the spectrally uncorrelated biphoton state and the heralded pure-state single-photon source from 14 isomorphs of the "KDP family". It is shown that 11 kinds of crystals, namely KDP, DKDP, ADP, DADP, ADA, DADA, RDA, DRDA, RDP, DRDP, and KDA still maintain the characteristics of KDP. For instance, they can satisfy three kinds of GVM conditions from near infrared to telecom bands, can prepare the spectrally uncorrelated biphoton state with purity as high as 0.98, and can achieve a visibility of 98% in the HOM interference between two independent heralded pure-state single-photon sources. Our work will provide good single-photon sources for photonic quantum information from near-infrared to telecom wavelength.

ACKNOWLEDGMENTS

This work is partially supported by the National Key R&D Program of China (Grant No. 2018YFA0307400), the National Natural Science Foundations of China (Grants No. 91836102, 11704290, 61775025, 61405030, 11104210), and by the Program of State Key Laboratory of Quantum Optics and Quantum Optics Devices (Grant No. KF201813), the fund from the Educational Department of Hubei Province, China (Grant No. D20161504) and the open research fund of Key Lab of Broadband Wireless Communication and Sensor Network Technology (Nanjing University of Posts and Telecommunications), Ministry of Education (Grant No. JZNY201709). We thank Guo-Qun Chen for helpful discussions.

[1] M. Grimau Puigibert, G. H. Aguilar, Q. Zhou, F. Marsili, M. D. Shaw, V. B. Verma, S. W. Nam, D. Oblak, and W. Tittel, Heralded Single Photons Based on Spectral Multiplexing and Feed-Forward Control, Phys. Rev. Lett. **119**, 083601 (2017).

[2] S. Liu, Q. Zhou, Z. Zhou, S. Liu, Y. Li, Y. Li, G. Guo, and B. Shi, Multiplexing heralded single-photon in orbital angular momentum space, arXiv:1810.03245 (2018).

[3] C. Joshi, A. Farsi, S. Clemmen, S. Ramelow, and A. L. Gaeta, Frequency multiplexing for quasi-deterministic heralded single-photon sources, Nat. Commun. **9**, 847 (2018).

[4] I. A. Walmsley and M. G. Raymer, Toward quantum-information processing with photons, Science **307**, 1733 (2005).

[5] M. A. Broome, A. Fedrizzi, S. Rahimi-Keshari, J. Dove, S. Aaronson, T. C. Ralph, and A. G. White, Photonic Boson sampling in a tunable circuit, Science **339**, 794 (2013).

[6] C. K. Hong, Z. Y. Ou, and L. Mandel, Measurement of Subpicosecond Time Intervals Between Two Photons by Interference, Phys. Rev. Lett. **59**, 2044 (1987).

[7] P. J. Mosley, J. S. Lundeen, B. J. Smith, P. Wasylczyk, A. B. U'Ren, C. Silberhorn, and I. A. Walmsley, Heralded Generation of Ultrafast Single Photons in Pure Quantum States, Phys. Rev. Lett. **100**, 133601 (2008).

[8] R.-B. Jin, J. Zhang, R. Shimizu, N. Matsuda, Y. Mitsumori, H. Kosaka, and K. Edamatsu, High-visibility nonclassical interference between intrinsically pure heralded single photons and photons from a weak coherent field, Phys. Rev. A **83**, 031805 (2011).

[9] R.-B. Jin, R. Shimizu, F. Kaneda, Y. Mitsumori, H. Kosaka, and K. Edamatsu, Entangled-state generation with an intrinsically pure single-photon source and a weak coherent source, Phys. Rev. A **88**, 012324 (2013).

[10] R. Valivarthi, M. G. Puigibert, Q. Zhou, G. H. Aguilar, V. B. Verma, F. Marsili, M. D. Shaw, S. W. Nam, D. Oblak, and W. Tittel, Quantum teleportation across a metropolitan fibre network, Nat. Photon. **10**, 676 (2016).

[11] R. Valivarthi, Q. Zhou, C. John, F. Marsili, V. B. Verma, M. D. Shaw, S. W. Nam, D. Oblak, and W. Tittel, A cost-effective measurement-device-independent quantum key distribution system for quantum networks, Quantum Sci. Technol. **2**, 04LT01 (2017).

[12] H.-K. Lo, M. Curty, and B. Qi, Measurement-Device-Independent Quantum Key Distribution, Phys. Rev. Lett. **108**, 130503 (2012).

[13] E. Meyer-Scott, N. Montaut, J. Tiedau, L. Sansoni, H. Herrmann, T. J. Bartley, and C. Silberhorn, Limits on the heralding efficiencies and spectral purities of spectrally filtered single photons from photon-pair sources, Phys. Rev. A **95**, 061803 (2017).

[14] W. P. Grice, A. B. U'Ren, and I. A. Walmsley, Eliminating frequency and space-time correlations in multiphoton states, Phys. Rev. A **64**, 063815 (2001).

[15] F. König and F. N. C. Wong, Extended phase matching of second-harmonic generation in periodically poled $KTiOPO_4$ with zero group-velocity mismatch, Appl. Phys. Lett. **84**, 1644 (2004).

[16] K. Edamatsu, R. Shimizu, W. Ueno, R.-B. Jin, F. Kaneda, M. Yabuno, H. Suzuki, S. Nagano, A. Syouji, and K. Suizu, Photon pair sources with controlled frequency correlation, Prog. Inform. **8**, 19 (2011).

[17] T. Lutz, P. Kolenderski, and T. Jennewein, Toward a downconversion source of positively spectrally correlated and decorrelated telecom photon pairs, Opt. Lett. **38**, 697 (2013).

[18] T. Lutz, P. Kolenderski, and T. Jennewein, Demonstration of spectral correlation control in a source of polarization-entangled photon pairs at telecom wavelength, Opt. Lett. **39**, 1481 (2014).

[19] T. Li, S. Sakurai, K. Kasai, L. Wang, M. Watanabe, and Y. Zhang, Experimental observation of three-photon interference between a two-photon state and a weak coherent state on a beam splitter, Opt. Express **26**, 20442 (2018).

[20] P. G. Evans, R. S. Bennink, W. P. Grice, T. S. Humble, and J. Schaake, Bright Source of Spectrally Uncorrelated Polarization-Entangled Photons with Nearly Single-Mode Emission, Phys. Rev. Lett. **105**, 253601 (2010).

[21] T. Gerrits, M. J. Stevens, B. Baek, B. Calkins, A. Lita, S. Glancy, E. Knill, S. W. Nam, R. P. Mirin, R. H. Hadfield, R. S. Bennink, W. P. Grice, S. Dorenbos, T. Zijlstra, T. Klapwijk, and V. Zwiller, Generation of degenerate, factorizable, pulsed squeezed light at telecom wavelengths, Opt. Express **19**, 24434 (2011).

[22] A. Eckstein, A. Christ, P. J. Mosley, and C. Silberhorn, Highly Efficient Single-Pass Source of Pulsed Single-Mode Twin Beams of Light, Phys. Rev. Lett. **106**, 013603 (2011).

[23] R.-B. Jin, K. Wakui, R. Shimizu, H. Benichi, S. Miki, T. Yamashita, H. Terai, Z. Wang, M. Fujiwara, and M. Sasaki, Nonclassical interference between independent intrinsically pure single photons at telecommunication wavelength, Phys. Rev. A **87**, 063801 (2013).

[24] Z.-Y. Zhou, Y.-K. Jiang, D.-S. Ding, and B.-S. Shi, An ultra-broadband continuously-tunable polarization-entangled photon-pair source covering the C+L telecom bands based on a single type-II PPKTP crystal, J. Mod. Opt. **60**, 720 (2013).

[25] R.-B. Jin, R. Shimizu, K. Wakui, M. Fujiwara, T. Yamashita, S. Miki, H. Terai, Z. Wang, and M. Sasaki, Pulsed Sagnac polarization-entangled photon source with a PPKTP crystal at telecom wavelength, Opt. Express **22**, 11498 (2014).

[26] M. M. Weston, H. M. Chrzanowski, S. Wollmann, A. Boston, J. Ho, L. K. Shalm, V. B. Verma, M. S. Allman, S. W. Nam, R. B. Patel, S. Slussarenko, and G. J. Pryde, Efficient and pure femtosecond-pulse-length source of polarization-entangled photons, Opt. Express **24**, 10869 (2016).

[27] M.-M. Wang, R.-A. Quan, Z.-Y. Tai, F.-Y. Hou, T. Liu, S.-G. Zhang, and R.-F. Dong, Measurement of the spectral properties of the coincident-frequency entangled biphoton state at optical communication wavelength (in Chinese), Acta Phys. Sin. **63**, 194206 (2014).

[28] N. Bruno, A. Martin, T. Guerreiro, B. Sanguinetti, and R. T. Thew, Pulsed source of spectrally uncorrelated and indistinguishable photons at telecom wavelengths, Opt. Express **22**, 17246 (2014).

[29] R.-B. Jin, M. Fujiwara, R. Shimizu, R. J. Collins, G. S. Buller, T. Yamashita, S. Miki, H. Terai, M. Takeoka, and M. Sasaki, Detection-dependent six-photon Holland-Burnett state interference, Sci. Rep. **6**, 36914 (2016).

[30] R.-B. Jin and R. Shimizu, Extended Wiener-Khinchin theorem for quantum spectral analysis, Optica **5**, 93 (2018).

[31] C. Greganti, P. Schiansky, I. A. Calafell, L. M. Procopio, L. A. Rozema, and P. Walther, Tuning single-photon sources for telecom multi-photon experiments, Opt. Express **26**, 3286 (2018).

[32] Z.-Y. Zhou, S.-K. Liu, S.-L. Liu, Y.-H. Li, Y. Li, C. Yang, Z.-H. Xu, G.-C. Guo, and B.-S. Shi, Revealing the Behavior of Photons in a Birefringent Interferometer, Phys. Rev. Lett. **120**, 263601 (2018).

[33] R.-B. Jin, T. Saito, and R. Shimizu, Time-Frequency Duality of Biphotons for Quantum Optical Synthesis, Phys. Rev. Appl. **10**, 034011 (2018).

[34] R.-B. Jin, R. Shiina, and R. Shimizu, Quantum manipulation of biphoton spectral distributions in a 2D frequency space toward arbitrary shaping of a biphoton wave packet, Opt. Express **26**, 21153 (2018).

[35] E. Meyer-Scott, N. Prasannan, C. Eigner, V. Quiring, J. M. Donohue, S. Barkhofen, and C. Silberhorn, High-performance source of indistinguishable entangled photon pairs based on hybrid integrated-bulk optics, arXiv:1807.10092 (2018).

[36] H. Terashima, S. Kobayashi, T. Tsubakiyama, and K. Sanaka, Quantum interferometric generation of polarization entangled photons, Sci. Rep. **8**, 15733 (2018).
[37] R.-B. Jin, R. Shimizu, K. Wakui, H. Benichi, and M. Sasaki, Widely tunable single photon source with high purity at telecom wavelength, Opt. Express **21**, 10659 (2013).
[38] A. M. Brańczyk, A. Fedrizzi, T. M. Stace, T. C. Ralph, and A. G. White, Engineered optical nonlinearity for quantum light sources, Opt. Express **19**, 55 (2011).
[39] P. B. Dixon, J. H. Shapiro, and F. N. C. Wong, Spectral engineering by Gaussian phase-matching for quantum photonics, Opt. Express **21**, 5879 (2013).
[40] A. Dosseva, L. Cincio, and A. M. Brańczyk, Shaping the joint spectrum of down-converted photons through optimized custom poling, Phys. Rev. A **93**, 013801 (2016).
[41] J.-L. Tambasco, A. Boes, L. G. Helt, M. J. Steel, and A. Mitchell, Domain engineering algorithm for practical and effective photon sources, Opt. Express **24**, 19616 (2016).
[42] C. Chen, C. Bo, M. Y. Niu, F. Xu, Z. Zhang, J. H. Shapiro, and F. N. C. Wong, Efficient generation and characterization of spectrally factorable biphotons, Opt. Express **25**, 7300 (2017).
[43] B. J. Smith, P. Mahou, O. Cohen, J. S. Lundeen, and I. A. Walmsley, Photon pair generation in birefringent optical fibers, Opt. Express **17**, 23589 (2009).
[44] B. Fang, O. Cohen, J. B. Moreno, and V. O. Lorenz, State engineering of photon pairs produced through dual-pump spontaneous four-wave mixing, Opt. Express **21**, 2707 (2013).
[45] R.-B. Jin, P. Zhao, P. Deng, and Q.-L. Wu, Spectrally Pure States at Telecommunications Wavelengths from Periodically Poled $MTiOXO_4$ (M = K, Rb, Cs; X = P, As) crystals, Phys. Rev. Appl. **6**, 064017 (2016).
[46] F. Laudenbach, R.-B. Jin, C. Greganti, M. Hentschel, P. Walther, and H. Hubel, Numerical Investigation of Photon-Pair Generation in Periodically Poled $MTiOXO_4$ (M = K, Rb, Cs; X = P, As), Phys. Rev. Appl. **8**, 024035 (2017).
[47] R.-B. Jin, G.-Q. Chen, F. Laudenbach, S. Zhao, and P.-X. Lu, Thermal effects of the quantum states generated from the isomorphs of PPKTP crystal, Opt. Laser Technol. **109**, 222 (2019).
[48] V. G. Dmitriev, G. G. Gurzadyan, and D. N. Nikogosyan, *Handbook of Nonlinear Optical Crystals* (Springer-Verlag, Berlin Heidelberg, 1999), 3rd ed.
[49] D. N. Nikogosyan, *Nonlinear Optical Crystals: A Complete Survey* (Springer-Verlag, New York, 2005).
[50] P. J. Mosley, J. S. Lundeen, B. J. Smith, and I. A. Walmsley, Conditional preparation of single photons using parametric downconversion: A recipe for purity, New J. Phys. **10**, 093011 (2008).
[51] See Supplemental Material at http://link.aps.org/supplemental/10.1103/PhysRevApplied.11.034067 for the original Mathematica codes, which show the details of the calculation.
[52] A. Smith, SNLO, http://www.as-photonics.com/snlo.
[53] F. Kaneda, K. Garay-Palmett, A. B. U'Ren, and P. G. Kwiat, Heralded single-photon source utilizing highly nondegenerate, spectrally factorable spontaneous parametric downconversion, Opt. Express **24**, 10733 (2016).
[54] E. Saglamyurek, N. Sinclair, J. Jin, J. A. Slater, D. Oblak, F. Bussieres, M. George, R. Ricken, W. Sohler, and W. Tittel, Broadband waveguide quantum memory for entangled photons, Nature **469**, 512 (2011).
[55] R.-B. Jin, T. Gerrits, M. Fujiwara, R. Wakabayashi, T. Yamashita, S. Miki, H. Terai, R. Shimizu, M. Takeoka, and M. Sasaki, Spectrally resolved Hong-Ou-Mandel interference between independent photon sources, Opt. Express **23**, 28836 (2015).
[56] H. Takesue, Entangled photon pair generation using silicon wire waveguides, IEEE J. Sel. Top. Quantum Electron. **18**, 1722 (2012).
[57] J. B. Spring, P. L. Mennea, B. J. Metcalf, P. C. Humphreys, J. C. Gates, H. L. Rogers, C. Söller, B. J. Smith, W. S. Kolthammer, P. G. R. Smith, and I. A. Walmsley, Chip-based array of near-identical, pure, heralded single-photon sources, Optica **4**, 90 (2017).
[58] X. Ren, D. Xu, and D. Xue, Crystal growth of KDP, ADP, and KADP, J. Cryst. Growth **310**, 2005 (2008).
[59] N. Sangouard, C. Simon, H. de Riedmatten, and N. Gisin, Quantum repeaters based on atomic ensembles and linear optics, Rev. Mod. Phys. **83**, 33 (2011).
[60] Q. Zhang, F. Xu, Y.-A. Chen, C.-Z. Peng, and J.-W. Pan, Large scale quantum key distribution: challenges and solutions [invited], Opt. Express **26**, 24260 (2018).
[61] R. J. Collins, R. Amiri, M. Fujiwara, T. Honjo, K. Shimizu, K. Tamaki, M. Takeoka, M. Sasaki, E. Andersson, and G. S. Buller, Experimental demonstration of quantum digital signatures over 43 dB channel loss using differential phase shift quantum key distribution, Sci. Rep. **7**, 3235 (2017).
[62] J.-Y. Hu, B. Yu, M.-Y. Jing, L.-T. Xiao, S.-T. Jia, G.-Q. Qin, and G.-L. Long, Experimental quantum secure direct communication with single photons, Light: Sci. Amp. **5**, e16144 (2016).
[63] R.-B. Jin, M. Takeoka, U. Takagi, R. Shimizu, and M. Sasaki, Highly efficient entanglement swapping and teleportation at telecom wavelength, Sci. Rep. **5**, 9333 (2015).
[64] S. Wengerowsky, S. K. Joshi, F. Steinlechner, H. Hubel, and R. Ursin, An entanglement-based wavelength-multiplexed quantum communication network, Nature **564**, 225 (2018).
[65] J. J. De Yoreo, A. K. Burnham, and P. K. Whitman, Developing KH_2PO_4 and KD_2PO_4 crystals for the world's most power laser, Int. Mater. Rev. **47**, 113 (2002).
[66] D. C. Burnham and D. L. Weinberg, Observation of Simultaneity in Parametric Production of Optical Photon Pairs, Phys. Rev. Lett. **25**, 84 (1970).